Journal of Wind Engineering & Industrial Aerodynamics 239 (2023) 105456

Contents lists available at ScienceDirect

Journal of Wind Engineering & Industrial Aerodynamics

journal homepage: www.elsevier.com/locate/jweia

Performance of asphalt shingles under simulated hurricane winds and evaluation of current installation practices

Ameyu B. Tolera [a,*], Ming Shiao [b], Arindam Gan Chowdhury [a,c], Ioannis Zisis [a,c], Peter Irwin [c]

[a] Department of Civil and Environmental Engineering, Florida International University, Miami, FL, USA
[b] GAF Materials Corp, Parsippany, NJ, USA
[c] Extreme Events Institute of International Hurricane Research Center, Florida International University, Miami, FL, USA

ARTICLE INFO

Keywords:
Asphalt shingles
Failure assessment
Installation methods
Full-scale experiment
Wall of Wind

ABSTRACT

This paper investigates the wind resistance of asphalt shingles, evaluates the efficiency of their current installation methods, and addresses the lack of a system-level resistance metric from a wind engineering standpoint. The study examined the wind performance of asphalt shingles considering three installation practices recommended in high-velocity wind areas and three nailing non-conformities due to workmanship issues by conducting full-scale failure assessment tests at the NHERI Wall of Wind Experimental Facility. Roofing Application Standard (RAS) No. 115 and FEMA's recommended practices, with and without modifications, were used as recommended practices; while missing nails, over-driven nailing, and high-nailing cases were simulated as installation deviations or errors. Monoslope, gable, and hip roof decks were also used to study the contribution of roofing geometries. The results showed that asphalt shingles installed using methods recommended by the current guidelines may be vulnerable to wind flows from critical directions. Asphalt shingles, tested in the current work, experienced failure at wind speeds below their design level, especially due to cavity pressurization. Nailing non-conformities were also observed to compromise shingles' performance. Additionally, asphalt shingle failure modes, extents, and areas varied with roof geometries and the employed installation methods.

1. Introduction

Low-rise residential buildings are vulnerable to damage during high-wind events. This can be attributed to their lightweight, vast abundance, and construction methods. Wind damage to these structures can be due to failures either in their structural system and/or the envelope itself. Recent hurricanes have revealed an improvement in the wind performance of their structural systems due to advancements in building codes and guidelines (Amini and Memari, 2020; FEMA, 2018, 2020). On the other hand, the wind resistance of building envelope systems and components still struggles to meet the load demand (Amini and Memari, 2020; FEMA, 2018, 2020). A loss of building components during wind events causes (1) a breach of the building envelope resulting in increased structural loads, (2) water intrusion damage to the interior of buildings, and (3) flying wind-borne debris that can put people and the built environment downstream at risk. Among the components of the building envelope, the failure of roofing elements was observed to be the major contributor to insured losses due to wind damage in residential buildings (Baheru et al., 2015; Cochran and Levitan, 1994; Gurley and Masters, 2011; van de Lindt et al., 2007).

This experimental study focuses on the wind resistance of asphalt composition shingles, the most widely used residential roofing material in North America. They have been the most popular form of residential roof covering in North America for over a century and are used in more than 80% of new construction and reroofing projects (ARMA, 2017; Dixon, 2013; Noone and Blanchard, 1993). This is credited to their effective water-proofing performance for steep-slope roofs; economical installation and life cycle cost; ease of installation; varied aesthetics and sustainability. The study of the wind loading, and resistance of asphalt shingles would therefore be beneficial to the resilience of the built environment.

1.1. Wind damage to asphalt shingles during previous hurricanes

Wind damage to asphalt shingles has been consistently reported in several reconnaissance surveys such as those conducted by Federal Emergency Management Agency (FEMA) (FEMA, 2004, 2005, 2006, 2009, 2018, 2019, 2020), Insurance Institute for Business and Home

* Corresponding author.
E-mail address: atole066@fiu.edu (A.B. Tolera).

https://doi.org/10.1016/j.jweia.2023.105456
Received 27 July 2022; Received in revised form 8 May 2023; Accepted 12 May 2023
Available online 26 May 2023

Safety (IBHS, 2004, 2009; Liu et al., 2010), and Roofing Industry Committee on Weather Issues (RICOWI, 2006, 2007, 2009, 2018a; b). The damage observations thereon can be grouped into four categories. The first is the widespread asphalt shingle damage observed during previous hurricane wind events that were below the design level adopted in the coastal areas. Hurricane Irma in 2017, for example, was such a below-design-level wind event for which severe shingle damage was observed (FEMA, 2018). Fig. 1a, b shows shingle damage on an elevated residential house in the Big Coppitt Key (FL) and a two-story residential house in Marathon (FL) for which the estimated 3-s gust wind speeds (EWS) at 10 m (33 ft) height were 49.6 m/s (111 mph) and 53.6 m/s (120 mph), respectively. Such speeds are lower than the 80.5 m/s (180 mph) 3-s gust design wind speed at 10 m height over open terrain for both these regions (ASCE, 2022; Florida Building Code, 2020). Note that, currently, the usage of asphalt shingles is limited to a mean roof height of 10 m (Florida Building Code, 2020).

The second consistent theme is that asphalt roofing shingle failures were observed for both new and old construction alike. Both residential houses in Fig. 1 were post-Florida Building Code (FBC) constructions, built in 2005 and 2007, respectively (i.e., after the state adopted one of the most stringent building codes in 2002 following the massive damage sustained due to Hurricane Andrew in 1992). These observations were consistent with reports from other post-FBC hurricane wind events. Even though the failures were more pronounced for older homes, similar below-design-level wind failure of asphalt shingles in newer construction is also indicative of persistent challenges in the wind resistance of these roofing elements.

The third observation pertains to the location of shingle failure. The reconnaissance teams reported that failure of hip and ridge trim shingles, and failures along the eaves and rakes were prevalent. These failure areas pertain to expected high suction locations on roofs, where wind flow separations are to occur due to discontinuities. Moreover, ridge-cap shingle failures often included ridge vent failures which resulted in significant water intrusion. Fig. 2 (a, b) shows such a case where only shingles at the roof ridge were lost and ridge vents allowed water ingress and the collapse of ceilings in multiple rooms. Shingles along roof eaves have also be observed to have been blown off, as shown in Fig. 3a, b, from Hurricane Harvey (2017) in Texas (FEMA, 2019). Fig. 4a, b shows gable end shingle failures from hurricanes Katrina and Charley (FEMA, 2004, 2006). Furthermore, asphalt shingles on hip roofs were reported to have performed better than those on gable roofs, showing wind performance variation with roof geometry.

Finally, the fourth observation is that most shingle failures were attributed to poor installation and construction practices. For example, most hip and ridge-cap shingles found in debris piles from Hurricane Michael (2018) were reported to have had no sign of roofing cement applied to them (FEMA, 2020). There were also reported cases where portions of shingles were left unsealed. Fig. 5a shows a residential house built 3 years before Hurricane Michael that sustained damage only to its hip and ridge-cap shingles possibly due to unsealing of shingles (FEMA, 2020). Besides inadequate hand dabbing of adhesive material, incorrect application of the starter course in eave areas was also stated as another cause for shingle blowoff. Poor fastening practices were also major consistent observations reported to have affected shingle wind performance. Most fasteners were nailed higher than their appropriate location [see Fig. 5b], over-driven due to the usage of excessive pressure, or even missing in most cases.

Based on these observations, the reports recommended that code enforcement authorities should make inspections of these roof covering materials a priority. They also suggested that the widespread asphalt shingle loss, especially on post-FBC constructions, needs to be assessed by industry groups and academia to investigate the possible reasons why they were failing during below design-level-wind events. More specifically, FEMA (2020) suggested that *"research should attempt to determine whether these failures were the result of design, installation, testing, inspection, manufacturing, or other issues"*. To achieve so, *"new research is needed to assess the actual performance of roofing products and systems in order to improve material production and installation specifications"* (IBHS, 2009). The current work is aimed to address these major issues by focusing on knowledge gaps related to the installation and testing of asphalt shingles. The results of the study are also expected to help improve the inspection and codification of these roofing elements.

1.2. Wind loading on and resistance of asphalt shingles

Wind loads on permeable roofing systems, such as asphalt shingles, are generally a function of upstream flow conditions; building- and component-generated turbulence; and correlation between the pressure on their top and bottom surfaces (Hazelwood, 1981; Kramer et al., 1979). The asphalt shingle uplift model developed by Peterka et al. (1997) assumes that wind loading on asphalt shingles is mainly due to flow separation from the leading edge of shingles, thus mainly attributed to component-generated aerodynamics [see Fig. 6a]. Peterka et al. (1997) state that, as opposed to impervious components, roof suctions in the separation bubble do not provide enough uplift to cause a fully sealed shingle to fail. Therefore, according to this model, the initiation of shingle failure is expected to occur in flow reattachment areas, where such local flow separations are anticipated. The model also relates the near-surface wind speed fluctuations to the net peak pressure fluctuations based on the quasi-steady assumption. For conservative peak wind load estimation, the authors suggest the use of an upper bound peak speed-up factor (i.e., the ratio of peak near-surface wind speed and mean wind speed of the approaching flow) of 2.5 which was reported by Cochran et al. (1999). This model forms the basis for the American Society for Testing and Materials (ASTM) Standard Test Method for Wind Resistance of Asphalt Shingles (Uplift Force/Uplift Resistance Method)

(a) EWS = 49.6 m/s (b) EWS = 53.6 m/s

Fig. 1. Shingle damage during hurricane Irma (Source: FEMA, 2018).

(a) Recently reroofed post-FBC house (b) Ceiling collapse due to water ingress

Fig. 2. Ridge-cap and ridge vent failure during Hurricane Michael (Source: FEMA, 2020).

(a) Ridge-cap and eave shingle damage (b) Eave shingle damage

Fig. 3. Ridge-cap and eave shingle failure during Hurricane Harvey (Source: FEMA, 2019).

(a) (b)

Fig. 4. Gable shingle damage during Hurricanes (a) Katrina and (b) Charley (Source: FEMA, 2004, 2006).

Fig. 5. Observed installation deficiencies after Hurricane Michael (a) unsealed shingles; (b) high-nailing (Source: FEMA, 2020).

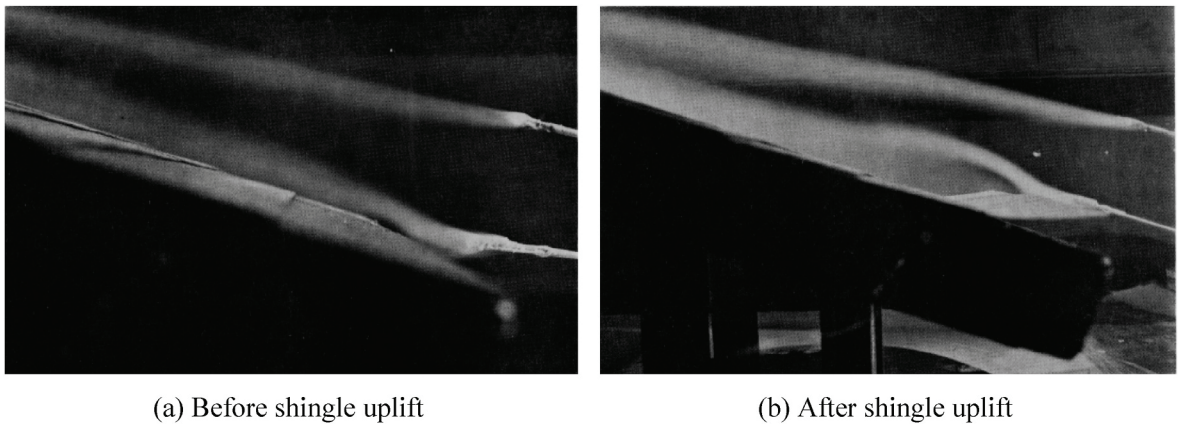

Fig. 6. Failure assessment test conducted by Peterka and Cermak (1983).

D7158 (ASTM International, 2020a). The test method measures uplift coefficients on the top and bottom surfaces of a shingle installed on a sloped panel. The instrumented shingle is situated in the center of the test panel to guarantee local flow separation at the leading edge. Peak uplift forces obtained from this test are then compared with the resistance obtained from ASTM D6381: Standard Test Method for Measurement of Asphalt Shingle Mechanical Uplift Resistance (ASTM International, 2020b). Besides ASTM D7158, the other standards used for evaluation and classification of the wind resistance of asphalt shingles by the FBC is ASTM D3161: Standard Test Method for Wind Resistance of Steep Slope Roofing Products (Fan-Induced Method) (ASTM International, 2020c). This test procedure involves conducting destructive tests by impinging a uniform jet of air onto a shingled panel for 2 h to record the failure wind speed (if failure occurs).

The wind resistance of asphalt shingles installed on actual roofs is not only attributed to the wind resistance of the individual shingle elements but is dependent on other components of the roof system, such as mechanical fasteners and roofing adhesives, and their integration (FEMA, 2010). Therefore, the wind performance of asphalt shingles, as tested by the previously discussed standardized tests, may not be representative of their performance on an actual roof during high wind events. Realistic estimation of the wind resistance on roofs should consider a holistic approach to address this cumulative effect. The state-of-the-art to perform this is by conducting more realistic failure assessment experimental tests which examine the entirety of the roof system (Chowdhury et al., 2009; Kopp et al., 2012; Leatherman et al., 2007). This type of testing method is also important to identify loading mechanisms that are not captured by aerodynamic tests. During aerodynamic wind load evaluation, the models are often tested at wind speeds that do not result in any damage to the building components and are kept in their intended functional position to the best of the examiners' abilities. There have also been cases where studies introduce techniques to model irregularities due to wind effects. Derickson et al. (1993), for example, added toothpicks to create gaps between shingle layers which were reported to increase pressure within the cavity behind the sealing strip. ASTM D7158 also instructs the insertion of shims that have a thickness of 1.0 mm under the leading edge of shingles to evaluate wind loads on slightly lifted cases (ASTM International, 2020a). These examples imply that localized and seemingly small changes in the shingle layout may result in significant changes in the uplift pressure. Furthermore, damage areas may not necessarily coincide with critical cases predicted from aerodynamic tests and could rather occur in weaker components or high fatigue areas. This highlights the importance of conducting failure assessment tests as they can capture complex wind-structure interactions which could lead to unforeseen failures of components and progressive damages resulting in the identification of weak spots and associated failure modes (Chowdhury et al., 2009; Kopp et al., 2012; Leatherman et al., 2007).

Wind tunnel destructive testing of asphalt shingles started by conducting blowoff tests using an impinging jet of air onto a shingled panel at a uniform wind speed and for certain durations, similar to ASTM D3168 (ASTM International, 2020c; Benjamin and Bono, 1967; Dixon et al., 2013). Peterka and Cermak (1983) identified that these tests lack realistic simulation of the turbulence in the boundary layer flow and thus could lead to unconservative results. Following this, they conducted failure assessment tests by modeling realistic wind flows at the Wind Engineering and Fluids Laboratory boundary layer wind tunnel at Colorado State University (Peterka and Cermak, 1983). These tests

resulted in the identification of shingle level flow separation [see Fig. 6], which was later developed by Peterka et al. (1997) to the asphalt shingle uplift model discussed earlier. Fig. 6 (a, b) shows flow separation from the leading edge of asphalt shingles before and after shingle uplift, respectively. Later, Smith and Millen (1999)investigated the influence of nailing location on asphalt shingle uplift resistance using data obtained from experimental testing of fifty decks at the same facility. The authors reported that shingle performance varied with products selected and the workmanship employed. Dixon et al. (2014) conducted a more realistic failure assessment test at the Insurance Institute for Business & Home Safety's (IBHS) full-scale boundary layer test facility on 6:12 slope hip-gable roofs to study the effects of shingle unsealing. They reported that blowoff patterns observed in the field had similar patterns with the partially unsealed field shingle failures from their experiments. Estes et al. (2017) used an ASTM D3161 test apparatus to evaluate the sensitivity of asphalt shingle's uplift resistance to the roof slope and installation temperature at the IBHS Research Center. The authors reported that there was no observed influence of roof slope on the wind performance of asphalt shingles. In contrast, the authors stated that shingle wind performance was correlated to the weather condition during the curing stage of shingles and the orientation of the roof relative to the sun. Recently, Tolera et al. (2022) also conducted full-scale aerodynamic and failure assessment tests using an asphalt shingled monoslope roof at the Florida International University's Wall of Wind (WOW) Experimental Facility (EF). The study reported that asphalt shingles installed near the upper corners of the monoslope roof experienced uplift pressures to which they were neither designed nor tested. This has raised questions on the accuracy of the current standardized testing methods as adequate indicators of actual wind performance.

The current study evaluates the performance of asphalt shingles in high winds by modeling the entire roof system to capture both the component- and system-level wind effects. The dependence of their wind resistance on both roof geometry and applied installation methods are also studied by considering variations in both parameters. With regards to installation methods, the study considered the current code and manufacturers' recommended practices and some installation deviations which were speculated to have influenced asphalt shingle performance during previous hurricanes. The roof geometries used, and installation practices followed along with their deviations have been detailed in Section 2. The full-scale experimental methodology and adopted test protocols are also discussed. The results of the study are then presented in Section 3. Finally, the authors provide recommendations for testing and installation methods with the conclusion of the study.

2. Experimental methodology

Full-scale asphalt-shingled roof models were engulfed in simulated atmospheric boundary layer (ABL) flows at the 12-fan NSF-NHERI Wall of Wind (WOW) Experimental Facility (EF) at Florida International University (FIU). The WOW is a large-scale open-jet wind engineering experimental facility that can simulate wind speeds up to 70 m/s (157 mph), equivalent to a category 5 hurricane on the Saffir-Simpson scale. The flow field of the WOW is 4.3 m (14.1 ft) high, 6.1 m (20 ft) wide, and 9.8 m (32.2 ft) downstream of the contraction zone, and is conditioned with spires and roughness elements that can help generate the desired atmospheric boundary layer profile (Chowdhury et al., 2017, 2018). Fig. 7a and b shows the WOW intake and contraction zone (i.e., flow management box), respectively.

Fig. 8. Hip-gable roof at the WOW turntable.

2.1. Roof models

The study comprises two different types of roof decks, hip-gable, and monoslope roofs built in-house at the WOW. The dimensions for the hip-gable roofs are 4.26 m (14 ft) wide and 3.12 m (10.2 ft) long with a roof slope (θ) of 4/12 on the gable side, as shown in Fig. 8. This construction technique gives an economical opportunity for studying wind effects on both gable and hip roofs. The model dimensions of the monoslope were 4.1 m (13.4 ft) wide and 3.94 m (13 ft) long with a roof slope (θ) of 3/12 (see Fig. 9). After construction, the full-scale roof decks were covered with underlayment to prevent the ingress of wind-driven rain and were then shingled with Miami Dade-certified asphalt laminate shingles. The shingle roofs were installed by licensed roofing contractors and were naturally conditioned on-site at the WOW. Note that the newly-installed shingles were inspected to ensure they were fully sealed prior to wind testing.

(a) 12-fan Wall of intake (b) WOW contraction zone

Fig. 7. The 12-fan NSF-NHERI wall of wind experimental facility.

Fig. 9. Monoslope roof at WOW turntable.

2.2. Shingle installation

Meeting the desired objectives demands careful installation of shingles such that they are representative of those in practice, for both conforming and non-conforming cases. The FBC instructs the use of Roofing Application Standard (RAS) No. 115 for the installation of asphalt shingles (Florida Building Code, 2020) in areas designated as High-Velocity Hurricane Zone (HVHZ) – e.g., South Florida. The other guideline evaluated in this study is a method described by FEMA in their Home Builder's Guide to Coastal Construction hereafter addressed as FEMA's recommended practices (FEMA, 2010). The main difference between these two installation methods lies in rake edge detailing methods. Therefore, five roof models have been shingled using these two methods in this study to evaluate these recommended practices. In summary, these are (1) a monoslope and a hip-gable roof installed using RAS-115, (2) a similar pair installed using FEMA's recommended practice as is, and (3) a monoslope roof installed with additional workmanship details to FEMA's suggestions. Three roof models installed with their respective nailing non-conformities to these guidelines were also simulated. The eight deck configurations along with their installation details are shown in Table 1 in their testing order.

Cases 1a and 1b corresponding to monoslope and hip-gable decks, respectively, followed the RAS-115 installation as provided in the Florida Building Code. The standard instructs: *"at all intersections, eaves, rakes, valleys, and gable ends the shingles and starter strips shall be set in a minimum 8-inch-wide strip of approved flashing cement."* Based on this, roofing cement meeting the FBC code requirement was applied along the rake edge with a 2.54 cm (1in.) gap to the edges (see Fig. 10). These gaps were provided to avoid roofing cement melting down the drip edges and causing aesthetical issues, which is a common practice in the roofing industry. The application of the adhesives was followed by direct shingle installation with a slight roofing cement spread over to the headlaps.

Cases 3a and 3b corresponding to monoslope and hip-gable decks, respectively, were shingled based on the FEMA Recommendation, which added further detailing to strengthen the rake and gable edges of the models. Like the previous case, 203 mm (8 in.) roofing cement was applied along the rake and gable edges as shown in Fig. 11a. In these cases, the roofing cement was applied up to rake edges with no gap provided. Shingles were also applied with this roofing cement interlaced in their headlaps, which provides an additional seal for the cavity underneath the shingles (see Fig. 11b). FEMA recommends the application of 3 dabs of 25.4 mm (1 in.) roofing cement between these layers, as opposed to spreading out with a putty knife, as applied in this study. This method also leaves gaps between layers like RAS-115 which were avoided based on the examiners' recommendation. Moreover, starter shingles were also used along the rake edges.

Case 6, which was applied on a monoslope deck, followed a similar installation method as recommended by FEMA with some additional modifications. As shown in Fig. 12, 203 mm (8 in.) roofing cement was applied along the rake edges of the monoslope. In this case, shingles were installed with polyurethane hand seals interlaced in their headlaps. In addition to these, 6 nails per shingle, as suggested by FEMA and Florida Building Code, were used to fasten shingles along their upper edges (see Fig. 13b).

As discussed earlier, installation non-conformities were also simulated to study the effect of installation deviations from code and manufacturer's recommendations. The authors discussed various installation deviations with manufacturers and insurance companies, in addition to the reviews from reports discussed in subsection 1.1 to come up with a list of important deviations. Among these, the three most important deviations: (1) Missing nails (Case 2), (2) Overdriven nailing (Case 4), and (3) High-nailing (Case 5) were selected. The missing nails (i.e., Fig. 13c) case signifies shingles installed on a monoslope roof using three nails to simulate the absence of one out of the four nails used in Case 1 (i.

Table 1
Failure assessment models.

Case #	Configuration	Roof geometry	Nailing	Starter Shingle	Rake Edge Details
1a	Control 1	Monoslope	4 nails	No	RAS-115
1b	Control 1	Hip – gable	4 nails	No	RAS-115
2	Missing nailing	Monoslope	3 nails	No	RAS-115
3a	Control 2	Monoslope	4 nails	Yes	FEMA Recommendation
3b	Control 2	Hip – gable	4 nails	Yes	FEMA Recommendation
4	Overdriven nailing	Monoslope	4 nails	Yes	FEMA Recommendation
5	High-nailing	Monoslope	4 nails	Yes	FEMA Recommendation
6	Control 3	Monoslope	6 nails	Yes	FEMA Recommendation*

Note: * Additional workmanship details.

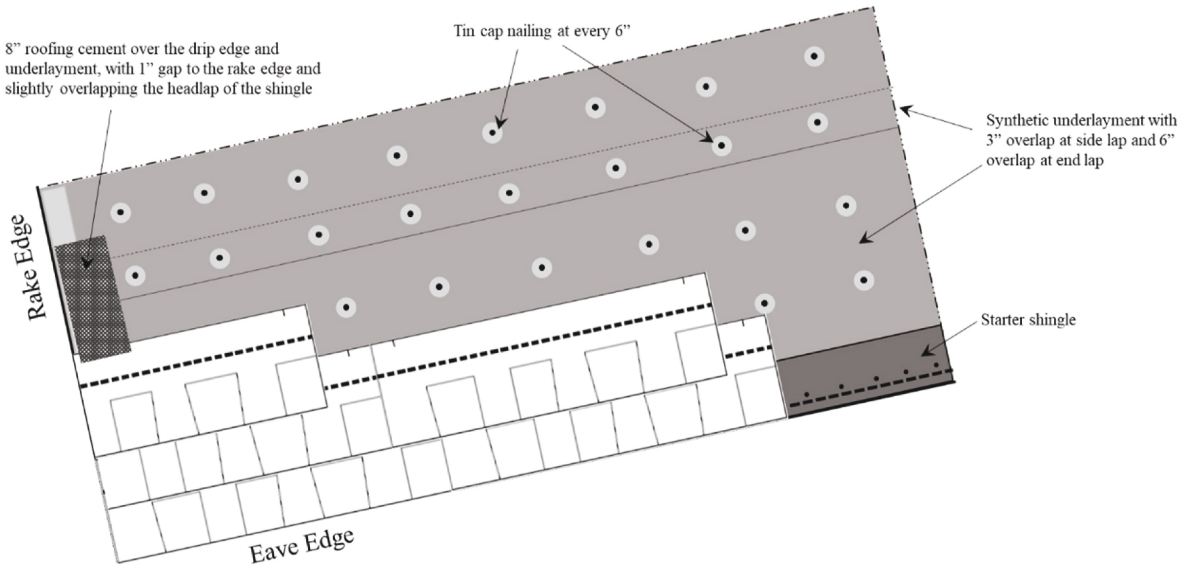

Fig. 10. Rake edge detailing for Cases 1 and 2.

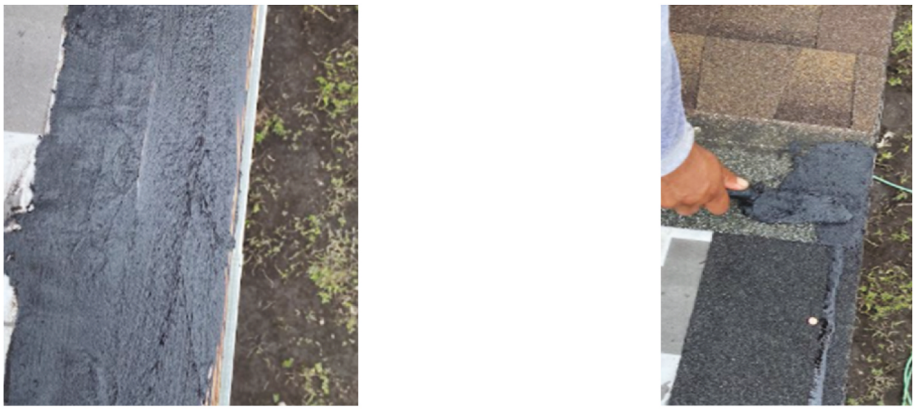

(a) Adhesive extending to the rake edge tip (b) Adhesive over the headlap

Fig. 11. Rake edge detailing for Cases 3, 4 and 5.

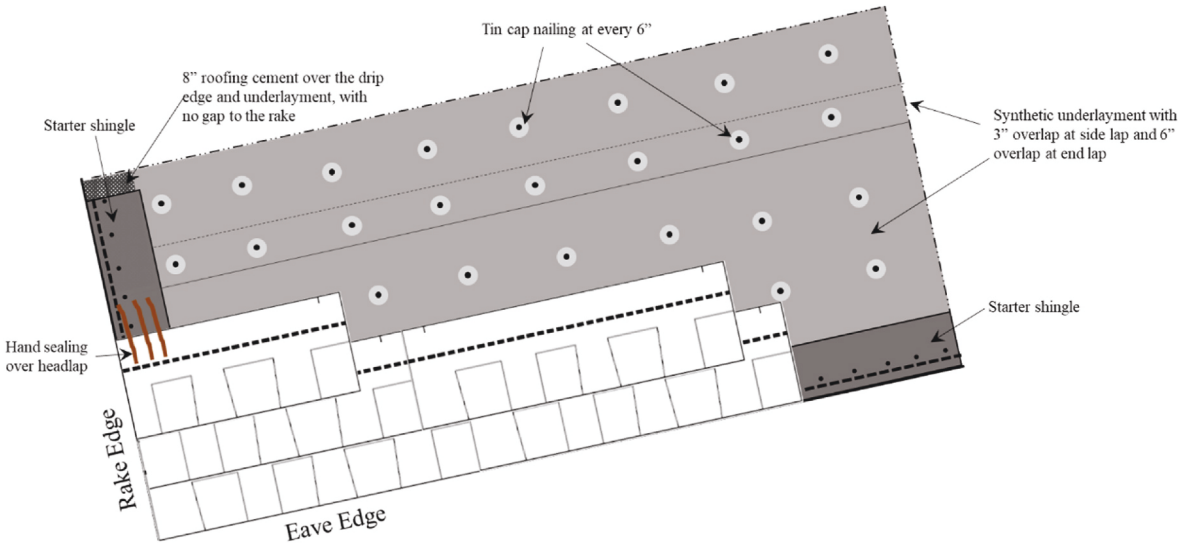

Fig. 12. Rake edge detailing for the third control Case 6.

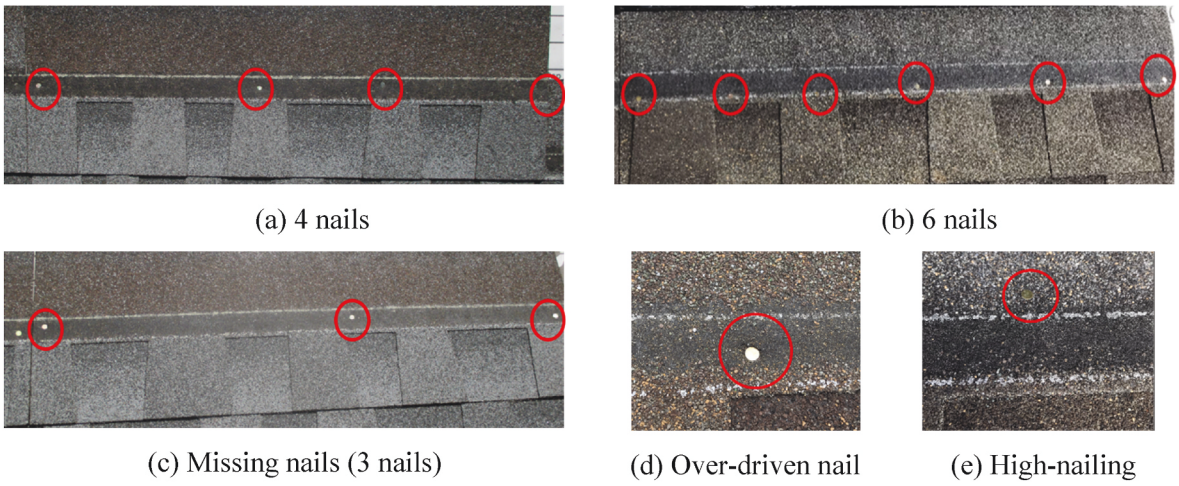

Fig. 13. Nailing configurations studied in the current work.

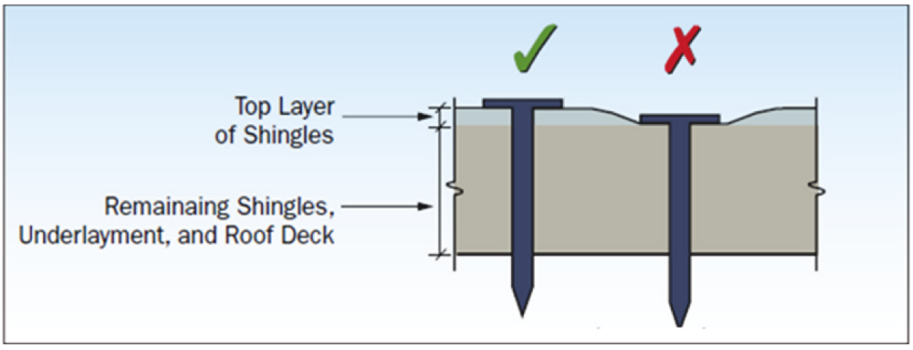

Fig. 14. Correctly and wrongly driven fasteners (FEMA, 2010).

e., Fig. 13a). Nails are to be applied straight into the plywood with the right amount of pressure to keep them flush with the shingle surface. This pertains to the first nail in Fig. 14. Application of excessive pressure would lead to overdriven nails where shingles are cracked and may be easily pulled through (the second nail in Fig. 14). This is the installation deviation studied here as an overdriven case as shown in Fig. 13d. Finally, nails are also expected to fall within the nailing region as is the case with all the nailing configurations shown in Fig. 13, except Fig. 13e. In this case, nails are applied higher than their normal location, falling behind the sealing strip of the top shingle, generally termed high-nailing. These installation deviations were incorporated into the installation methods discussed previously and were used on additional three monoslope roof decks, accordingly, as shown in Table 1.

2.3. Experimental test protocol

In this experiment, atmospheric boundary layer (ABL) wind flows were simulated for open terrain exposure with a roughness length zo =

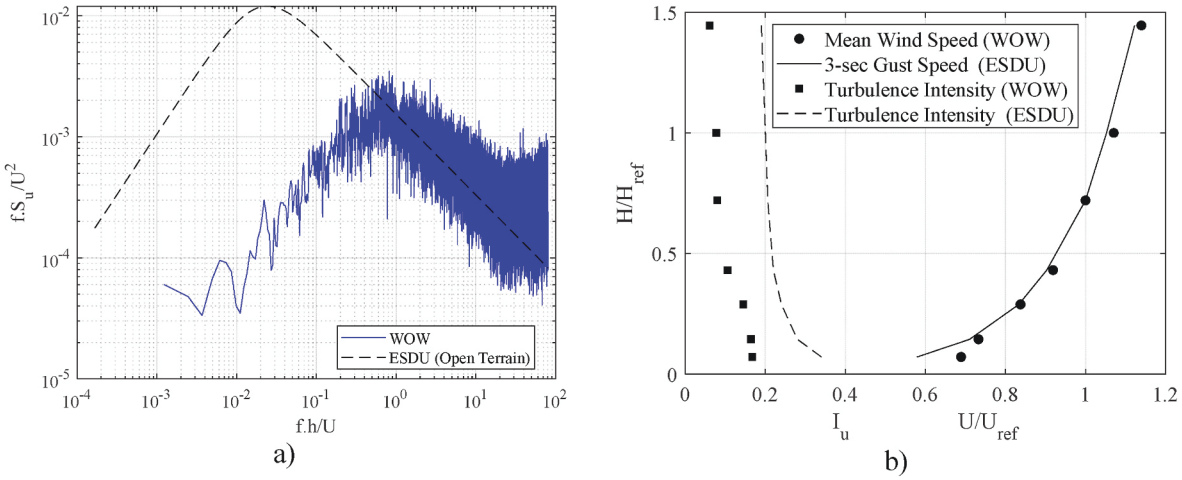

Fig. 15. (a) Von Karman and WOW wind spectra at mean roof height (b) open terrain profile.

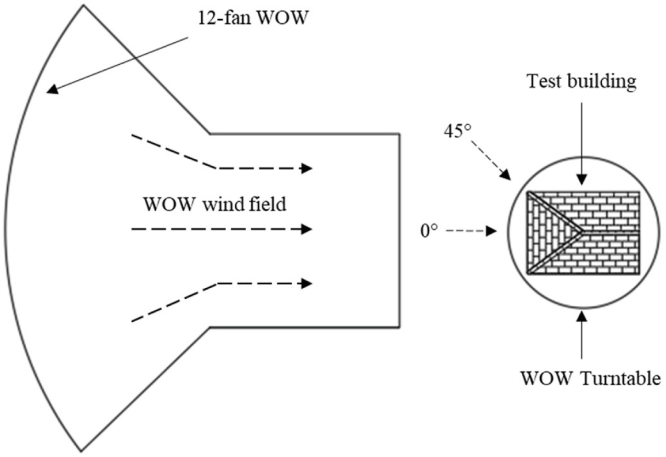

Fig. 16. Experimental setup at the WOW with the hip-gable roof on the turntable.

0.07m. To benefit from the full-scale testing, wind flow simulation at the WOW followed the partial turbulence simulation (PTS) approach, where only the high-frequency (i.e., small-scale) part of the wind turbulence spectrum is simulated (see Fig. 15a) as the length scale of the low-frequency eddies at full-scale extends beyond the height of the wind tunnel. Based on the PTS approach, the small-scale turbulence interacts directly with the turbulent shear layers and vortices that originate at the edges of the roof. The configurations and strengths of these shear layers and vortices directly affect the suctions on the roof surfaces and possibly cause local failures of building components (e.g., roof shingles in this study). The missing low-frequency (i.e., large-scale) component of the spectrum can be approximately treated similarly to changes in the mean flow velocity based on the quasi-steady aerodynamic theory (ASCE, 2021; Estephan et al., 2022; Mooneghi et al., 2016; Moravej, 2018). Note that the PTS approach followed during aerodynamic tests entails the simulation of the high-frequency component of the full spectrum at the wind tunnel and a post-test analytical analysis to compensate for the missing low-frequency component. However, during failure assessment tests, such compensation is not needed given that the component of the wind spectrum (small-scale turbulence) responsible for the failure of the building components of interest has been fully simulated in the experiments. At the WOW, the simulated high-frequency wind flow, at large model scales, consists of a sequence of eddies with gust durations of about 3-s each, and their mean wind speeds are comparable to 3-s gust ABL wind speeds [see Fig. 15b]. Therefore, testing for 60 s at the WOW implies subjecting the specimen to about twenty of these 3-s events, where each represents the highest 3 s of wind speed in 1 h. Moreover, since the usage of asphalt shingles is limited to a maximum mean roof height of 10 m (33 ft), the testing wind speeds from this study can be directly compared with the 3-s gust speed provided in ASCE 7–22 (ASCE, 2022).

In this study, wind flows were directed from orthogonal and oblique directions (i.e., 0°, 45°, 90°, 135°, and 180°) by rotating the full-scale models of all tested configurations counterclockwise on the WOW turntable. For the hip-gable model, 0° wind direction pertains to wind flows directed normally to the hip side as shown in Fig. 16 while for the monoslope roof, 0° is where wind flows are normal to the lower eave. The simulated 3-s mean roof height wind speeds ranged from 22.6 m/s (50.6 mph) to failure wind speeds with increments of 3.6 m/s (8 mph). Each wind speed was maintained for 60 s in each direction during which examiners monitored the state of the asphalt shingles using high-definition cameras before increasing to the next wind speed. After the failure of shingles is reached, post-mortem analysis was performed to investigate possible failure causes.

3. Results and discussion

This study focused on conducting high-speed destructive tests to determine the efficiency of the current asphalt shingle installation methods (i.e., objective 1), and the effects of installation deviations from code and manufacturer's recommendations on the wind resistance of asphalt shingles (i.e., objective 2). The observed failure causes during the destructive tests can be generalized into three predominant loading mechanisms. These are cavity pressurization, external roof surface suction, and combined action from these two forces. A detailed discussion of each case is presented hereafter. This is followed by an analysis of the effect of nailing non-conformities and the effect of roofing geometries. Results of this experimental campaign, detailed using spider charts, are included in Appendix A of this paper.

3.1. Failure due to cavity pressurization

The first control models (Cases 1a and 1b) and the missing nails case (Case 2) failed due to a predominant positive pressure buildup within their cavities. The failure was initiated along the rake and gable edges of the monoslope and gable roofs, respectively. In all three cases, the wind direction responsible for the shingle failure was a wind directed normally to the roof slope. Wind flows entered the cavity through the rake edge openings and caused shingle billowing at a 3-s wind speed of 34 m/s (76 mph). This is significantly lower than the design 3-s wind speed required by the FBC code or Miami Dade code, 80.5 m/s (180 mph). The external surface of these shingles was subject to suction due to wind separating from the rake and gable edges. However, it was the positive pressure build-up within the cavity that progressively started to cause ballooning and nail pull-through that expanded to the middle parts of the roof. This phenomenon can be expressed as pressure escalation or having a permeability factor higher than one as discussed by Tolera et al. (2022). Permeability factor, β, is the ratio of the net pressure P_{net} on asphalt shingles, which is the algebraic sum of the external surface pressure P_{ext} and cavity pressure P_{cav}, to the external surface pressure P_{ext} [see Equations (1) and (2)]. Based on this, $\beta > 1$ implies pressure escalation due to positive cavity pressure while $\beta < 1$ indicates pressure equalization due to negative cavity pressure. For detailed discussion, readers are referred to Tolera et al. (2022). The monoslope and gable models at the onset of shingle liftoff due to cavity pressurization are shown in Fig. 17a, b, respectively.

$$P_{net} = P_{ext} - P_{cav} \tag{1}$$

$$\beta = P_{net}/P_{ext} \tag{2}$$

These results showed that shingled roofs installed using the RAS-115 installation method may be susceptible to failures due to cavity pressurization along their rake edges, which may in part be due to insufficient rake edge sealing. As discussed earlier, it is a common practice to leave a gap of about 25.4 mm (1 in.) thick at the edges, as shown in Fig. 18a, to avoid the dripping of this adhesive along the drip edges, which would cause a call back for the contractor. Having as small as a 25.4 mm gap along these edges may provide sufficient cavity space for positive pressure to develop, implying that such practices may create a vulnerability in the roof system. Moreover, the lack of sufficient roofing cement between shingle layers in the headlap region can also provide a cavity space, as shown in Fig. 18b, for the development of positive pressure.

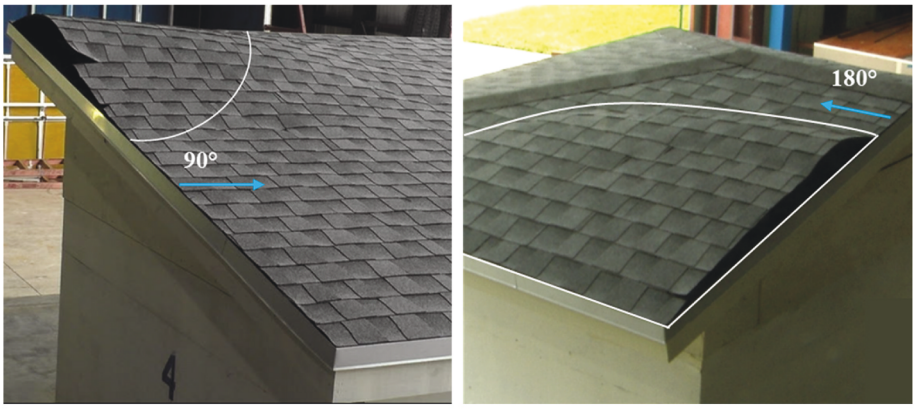

(a) (b)

Fig. 17. Ballooning due to positive cavity pressure for (a) Case 1a, and (b) Case 1b.

(a) (b)

Fig. 18. (a) Gap left at the rake edge; (b) Gap between shingle layers in the headlap.

(a) (b)

Fig. 19. Gable-end shingle failure mechanism for hip-gable roof Control 2b (a) shingle billowing in the interior parts of the roof, and (b) gable end shingle liftoff initiation.

Fig. 20. Case 6: shingle liftoff near the upper corner at a 3-s peak wind speed of (a) 49.2 m/s and (b) 53.2 m/s.

3.2. Failure due to a combination of suction and cavity pressurization

Results from the second control monoslope and hip-gable roofs (Cases 2a and 2b, respectively) installed using FEMA's recommended practices, showed an improved wind resistance. Shingle failures were observed at a 3-s peak wind speed of 41.6 m/s (93 mph) for both models – a 22% increase from the failure wind speed recorded for decks installed with RAS-115. A different loading mechanism was observed in this case. Shingle uplift due to wind flow separating from the rake edges were observed before any positive pressure buildup within the cavity. Shingles behind the roofing edge seal were observed to have been pulled through their fasteners due to this loading mechanism while the adhesives were still holding against entry of wind flow into the cavity, see Fig. 19a. Therefore, the loading mechanism was, first, predominantly due to the external surface suction, i.e., permeability factor lower than or about equal to unity. But soon after this, as the testing wind speed reached 41.6 m/s, the rake edge roofing adhesive seals opened, allowing wind flows to enter the cavity and develop positive pressure (see Fig. 19b). Once this stage is reached, the shingle failure mechanism changed from being driven by surface suction to cavity pressurization, resulting in an immediate failure.

3.3. Failure due to predominant roof suction

The added workmanship details discussed in subsection 2.2 for Control 3 (Case 6), resulted in further improvement in wind resistance. Loss of shingles was recorded at a 3-s wind speed of 56.8 m/s (127 mph) at mean roof height for a wind directed from the lower eave corner (i.e., testing wind direction of 45°), a 67% increase compared to those installed using RAS-115. The added rake edge detailing and increased number of nails were able to increase the failure wind speed by 37% compared to the monoslope installed with FEMA's recommended practices. Even though this installation method provided improved performance, the failure wind speed observed is still below the design wind speed required in HVHZs according to the FBC and ASCE 7–22 (ASCE, 2022; Florida Building Code, 2020). Moreover, failures happened in this wind direction because shingles were already lifted and were pulled through their fasteners by dominant wind directions, especially from those directed to the upper corners at lower wind speeds, as shown in Fig. 20 (a, b). These failures, consistent with the aerodynamic study conducted by Tolera et al. (2022), were initiated near the upper corner of the monoslope due to wind flow directed to these corners (135°). Moreover, the aerodynamic study also reported significant pressure equalization ($\beta < 1$) in the failure zone. Even though negative cavity pressures reduced the net pressure acting on the shingle, the external suctions were high enough to cause shingle uplift. Such failure modes are contrary to the basic assumption that shingle failures are initiated by local aerodynamics, mostly expected in flow reattachment areas (ASTM International, 2020a; Dixon et al., 2013; Peterka et al., 1997). Additionally, this installation method produced improved performance at the rake edge relative to the other installation techniques. Effectively securing the rake edges against cavity pressurization shifted the first place in which failure began from the rake edges to the upper corners (see Fig. 21), contrary to the two failure mechanisms discussed in subsections 3.1 and 3.2. Even though interior shingles located behind the rake edge adhesives were also pulled through their nails, these shingles were not blown off [see Fig. 21].

Fig. 21. Case 6: shingle blowoff at a 3-s peak wind speed of 56.8 m/s.

Fig. 22. Hip shingle lift at a 3-s peak wind speed of 38 m/s.

3.4. Dependence of shingle wind resistance on roof geometry and wind direction

The results from this study showed the significant dependence of the wind resistance of asphalt shingles on roof geometry and wind direction. As reported by Tolera et al. (2022), critical peak net wind loads on asphalt shingles followed the critical external loading conditions dictated by the roof geometry. As previously mentioned, blow-offs for Control 3 were initiated by shingles lifting near the upper corner of the monoslope likely due to conical vortices (Tolera et al., 2022). Hip roofs were found to provide better wind performance as reported in previous reconnaissance surveys (FEMA, 2018, 2019, 2020). The two hip-gable roofs tested, installed using RAS-115 and FEMA recommended practices, (i.e., Control 1b and Control 2b, respectively), did not incur any interior/field shingle failure on their hip sides. In contrast, hip trim shingles were observed to lift off prematurely due to a cornering wind at a 3-s mean roof height wind speed of 38 m/s (85 mph) as shown in the circled section of Fig. 22, highlighting the prevalence of hip trim shingle failure during high winds.

Furthermore, the wind resistance of asphalt shingles was also observed to be dependent on wind direction. Wind flows directed parallel to the roof slope (i.e., normal to the asphalt shingles' leading edge) presented the least loading conditions. These were consistent for all three roof geometries tested. Such wind flows exerted loads less than the wind resistance of the asphalt shingles, predominantly coming from the self-sticking bituminous adhesive. As classified by ASTM tests (D3161 and D7158), the shingles were suited for these types of loads at such wind speeds. The uplift model by Peterka et al. (1997), which assumes high net pressure in the reattachment areas as tested in ASTM D7158 [see Fig. 6a], may not be adequate for the critical loading condition. This implies that restricting shingle failure areas to flow reattachment zones leads to the overestimation of asphalt shingle resistance. It is, therefore, important to re-examine these assumptions.

3.5. Effect of nailing nonconformities

Installation deviations from code and manufacturer's recommendations considered in this study focused on nailing patterns. Besides the provision of 6 and 4 nails per shingle, as recommended by building codes and manufacturers, missing nails (i.e., 3 nails), over-driven nailing, and high-nailing were simulated and tested at the WOW, as discussed in subsection 2.2. The failure assessment results showed that nailing patterns affect the wind resistance of asphalt shingles significantly, especially for shingles placed away from the roof edges.

Asphalt shingles installed with a simulated missing nail case on a monoslope roof followed the RAS-115 installation procedure, except for the nailing pattern, and were therefore compared with those on Case 1b. From the comparison between these two cases, it was observed that rake edge detailing contributed more to the wind resistance of the shingles than did the nailing non-conformity. The failure wind speed was higher for the missing nails case compared to Control 1, but damage to the shingles happened at similar wind speeds, 34 m/s (76 mph). A comparison of shingle uplift over the entire roof surface between these two models showed that shingles installed with missing nails were prone to lifting under wind suctions. Intense uplift motion started from the early stages of the test for the case with missing nails compared to Control 1. This implies that if the missing nail case was installed using improved edge detailing similar to Control 3, the failure wind speed may have been different from the baseline.

The over-driven and high-nailing cases were installed using a similar installation method as Case 2b, except for their respective simulated deviations. These nailing non-conformities also made shingles more prone to lifting and failures but did not affect the shingle wind resistance as much as the rake edge detailing. The over-driven nailing case showed better resistance against shingle uplift at lower wind speeds. But at the advent of vibration, shingles were lifted immediately indicating easier nail pull-through, and they were blown off prematurely. In contrast, high-nailed shingles started vibrating early on. Shingles, in this case, tended to be the most lifted under the wind flow and responded to a greater number of wind directions than in the second control case. Again, the effects of these non-conforming nailing patterns would have been more significant if they were installed with the installation applied on Control 3 than the other two. Comparing the wind speeds at which shingle motion and shingle failure were observed for the over-driven and high-nailing cases with that of Control 3, it can be assumed that these two non-conformities may considerably reduce the failure wind speed. Similar observations may be made between the usage of 4 (i.e., the first and second control cases) and 6 (i.e., the third control case). The latter was observed to provide better resistance to shingle lifting and vibration.

Besides the importance of proper nailing practices, the destructive test results in the current study showed the importance of the mechanical property of asphalt shingles in their wind performance. As discussed earlier, failures attributed to cavity pressurization resulted due to wind flows entering the cavities and causing shingle pull-through, thus the ballooning of the roof cover. In addition to this, shingle blowoffs are often initiated by a failure of a single shingle that also causes the wind to enter the cavities. From these failure modes, it is apparent that, in addition to surface suction, shingle liftoff due to cavity pressurization and cascading failures because of adjacent shingle failures are mainly

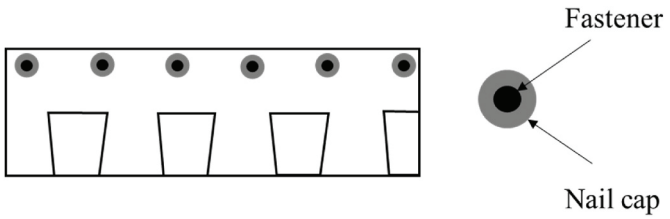

Fig. 23. Usage of nail caps to increase pull-through resistance of asphalt shingles.

Fig. 24. Gable end drip edge and fascia.

resisted by the fasteners. Moreover, these loads translate to the shingles as punching shear force that needs to be resisted by the mechanical property of the shingles. This can be observed from the relative performance between Case 3a (a properly driven one) and Case 4 (over-driven nailing). In the latter case, shingles were cracked around their fasteners and were easily pulled through their nails signifying a weaker punching shear resistance. However, currently, there are no performance metrics for the punching shear resistance of asphalt shingles, and they are not currently designed for such wind loads. To this end, the current study forwards two recommendations. The first is the development of new test protocols that investigate the punching shear resistance of asphalt shingles. The second recommendation is the usage of nail caps to increase shingle wind resistance against pull-through [see Fig. 23]. This is intended to reduce the stress on the shingles by increasing the contact surface area. In addition, this method could also help mitigate shingle cracking due to over-driven nailing. Future studies are encouraged to further investigate the wind resistance of asphalt shingle with and without the application of nail caps.

3.6. Drip edge failures

Drip edges are roof perimeter flashing elements mechanically fastened at the eaves, rakes, and gable ends to keep rainwater away from the fascia and from getting underneath roofing components [see Fig. 24]. In this study, drip edges were installed on all roof decks as directed by the FBC (2020). In all the models tested, drip edges were observed to vibrate significantly, especially in wind flows directed normal to their length. Although there was no intentional installation variation between the full-scale models, failure of drip edges was observed for those installed on Control 3. These failures occurred at a testing 3-s mean roof height wind speed of 38 m/s by wind flows directed to the upper corners (135°), which is significantly below their design wind speed as per the Florida Building Code (2020). Once these members were lifted, experiments were stopped to add mechanical fasteners normal to their surface to avoid any change to the wind loading or resistance of asphalt shingles. The wind performance of drip edges has not been investigated in this study as it is beyond its scope. However, the authors encourage future studies to examine the wind loading of these roofing elements.

4. Conclusion

Asphalt shingle failures have been observed during the past hurricane wind events, which were mostly attributed to poor installation practices. This study investigated the causes of shingle failures from a wind engineering standpoint by setting out two main objectives. The first was evaluating the efficiency of the current installation methods, for which RAS-115 and FEMA's recommended practices with and without modification were selected. The second objective was to measure the impact of three installation non-conformities: missing nails, over-driven nailing, and high-nailing. To meet these objectives, asphalt shingled monoslope and hip-gable roof decks were subjected to simulated open terrain atmospheric boundary layer flows to evaluate the wind performance of asphalt shingles.

The results highlighted the importance of installation methods in the wind performance of asphalt shingles, and that the current recommended practices may not provide the necessary resistance in high wind areas. Even though the shingles tested were certified for high wind zones, premature failures and blowoffs were recorded for shingles installed using the current recommended practices. In this study, full-scale models shingled using RAS-115 and FEMA's recommended practices were observed to be vulnerable to failure initiations from their rake/gable edges due to cavity pressurization. The provision of additional rake edge detailing was seen to significantly increase the failure wind speed. In this case, failure mechanisms shifted from cavity pressurization to suction on the upper surface of shingles located in high suction areas. Failure mechanisms noted in this experimental campaign were observed to be different from those tested using standardized tests such as ASTM due to the contribution of building size turbulence and installation methods. This implies that the current standardized tests may overestimate the wind resistance of asphalt shingles by neglecting critical loading cases.

Nailing non-conformities were observed to cause a reduction in wind resistance, although not as much as an inadequate rake and gable edge sealing. Lack of proper nailing made shingles more vulnerable to wind action, thus weakening them against wind loads. The provisions of 6 nails per shingle provided higher resistance against shingles lifting compared to fastening with 4 nails. As expected, missing nails increased uplift shingle motion. Similarly, over-driven nailing and high-nailing were observed to cause similar effects, where those of the former were more pronounced than the latter.

Future research should further study the wind resistance of asphalt shingles by addressing the two main limitations of the current work. The first limitation pertains to the size of the full-scale model used in the experiment. Even though the bluff body aerodynamics pertaining to the roof geometry is fully captured, there is a difference between the tested full-scale model and full-size family home. The difference lies in the fact that as the building size increases, the edge and field zones do not increase proportionally. The second limitation of the study is an inadequate sampling of simulated cases which may not be representative of the entire population. Future studies should also consider testing enough samples for each case to see if there is any variation from the current results.

CRediT authorship contribution statement

Ameyu B. Tolera: Conceptualization, Formal analysis, Methodology, Investigation, Writing – original draft, Writing – review & editing. **Ming Shiao:** Methodology, Investigation, Writing – review & editing. **Arindam Gan Chowdhury:** Conceptualization, Supervision, Resources,

Funding acquisition, Writing – review & editing. **Ioannis Zisis:** Conceptualization, Supervision, Resources, Funding acquisition, Writing – review & editing. **Peter Irwin:** Conceptualization, Supervision, Validation, Writing – review & editing.

Declaration of competing interest

The authors declare the following financial interests/personal relationships which may be considered as potential competing interests: Arindam Gan Chowdhury and Ioannis Zisis report financial support was provided by National Science Foundation Industry-University Cooperative Research Centers Program. Arindam Gan Chowdhury and Ioannis Zisis report additional financial support was provided by GAF Materials Corp. Ming Shiao reports a relationship with GAF Materials Corp that includes: employment.

Data availability

Data will be made available on request.

Acknowledgment

The study was funded by the National Science Foundation (NSF) through the Industry/University Cooperative Research Center (IUCRC) to the Wind Hazard Infrastructure Performance (WHIP) Center at Florida International University (FIU) (award numbers 1520853, 1841503, and 2037899). The authors would also like to thank GAF for providing additional support to cover the expenses of purchasing and installing all the materials needed for the experiment. The experiments were greatly facilitated by the fine work of WOW staff members Dr. Steven Diaz, Walter Conklin, Dr. Dejiang Chen, Roy Liu-Marques, James Erwin, and Manuel Matus. Ameyu Tolera gratefully acknowledges funding from the Florida International University Graduate School (FIU UGS) Dissertation Year Fellowship (DYF). The opinions, findings, conclusions, or recommendations expressed in this article are solely those of the authors and do not represent the opinions of the funding agencies.

Appendix A. Failure Assessment Results

The full-scale failure assessment test results have been showcased in this appendix using spider/radar charts. Seven performance parameters have been used to present these observations at each wind speed and direction. These parameters are (1) Shingle vibration, (2) Area shingle lifting, (3) Rake edge vibration, (4) Rake edge lifting, (5) Single shingle blowoff, (6) Roof section blowoff, and (7) Flashing lifting. The five radii of the radar plots represent the wind directions for which the shingled roofs were tested (0°–180° at 45° increments). The radii are connected to each other by six radar lines that signify performance levels ranging from 0 to 5. The interpretations of the performance levels are as follows.

1. Shingle vibration: describes the shingle's upward and downward movement visually ranked from 0 (no vibration observed) to 5 (maximum vibration) with no loss of shingles.
2. Area shingle lifting: describes the billowing of the roof and is used to measure what percentage of shingles became loose and were lifted up from the roof deck, creating an exposed gap or void underneath without being blown off. A performance level of 5 in this case represents a case where all shingles were lifted.
3. Rake edge vibration: like shingle vibration, this parameter describes the extent of shingle movement and is only limited to shingles installed along the rake edges.
4. Rake edge lifting: like area shingle lifting, this parameter describes what percentage of rake edge shingles have been lifted and have stayed up during the test duration.
5. Single shingle blowoff: is used to describe what percentage of shingles were missing or displaced, leaving the underlayment or roof deck exposed without causing adjacent shingles to be blown off.
6. Roof section blowoff: describes what percentage of the roof covering is detached and blown away from the roof deck.
7. Flashing lifting: describes what percentage of the flashing has been raised or lifted, creating a visible gap or space between the flashing and the roof surface.

A.1. Case 1a: Monoslope Control 1

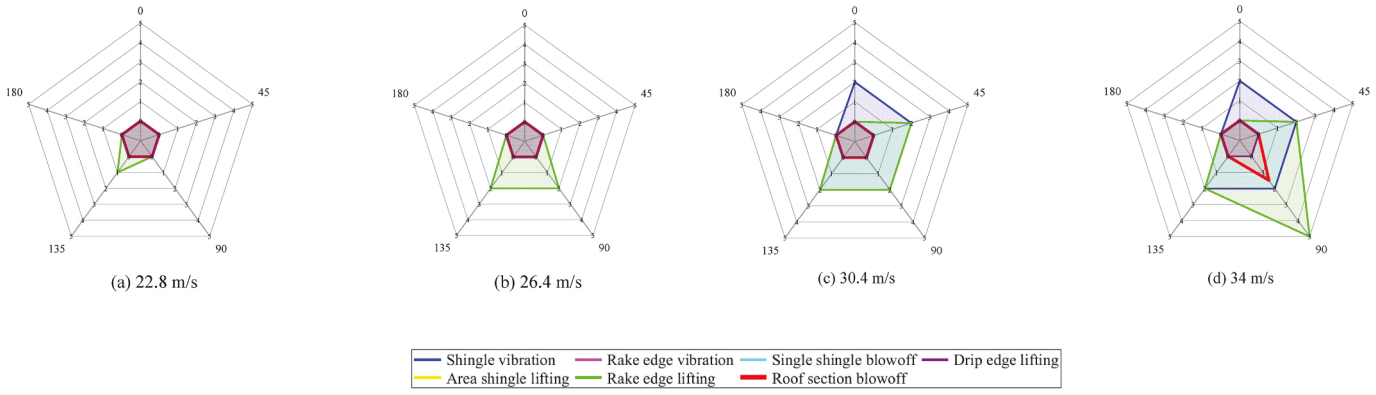

(a) 22.8 m/s (b) 26.4 m/s (c) 30.4 m/s (d) 34 m/s

A.2. Control 1b: Hip-gable Control 1

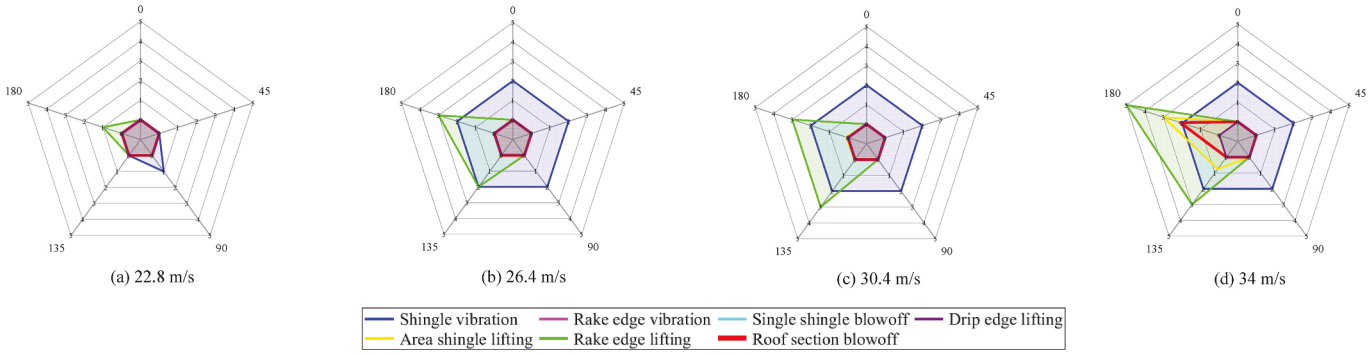

(a) 22.8 m/s (b) 26.4 m/s (c) 30.4 m/s (d) 34 m/s

A.3. Case 2: Missing Nails

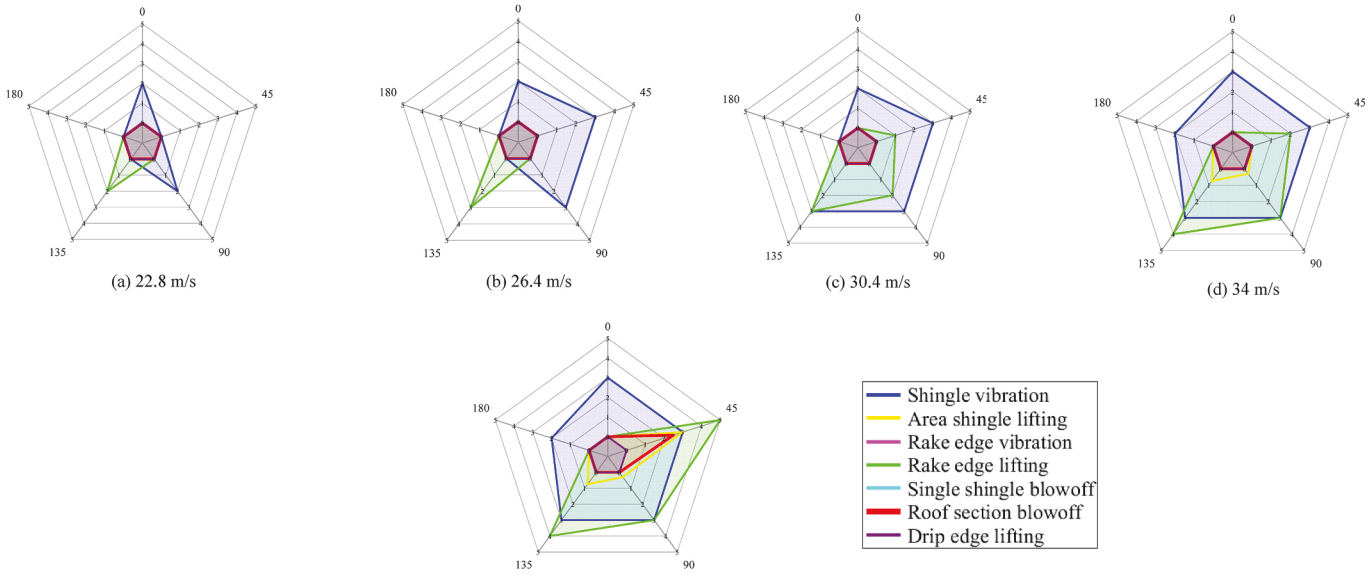

(a) 22.8 m/s (b) 26.4 m/s (c) 30.4 m/s (d) 34 m/s

(d) 38 m/s

A.4. Case 3a: Monoslope Control 2

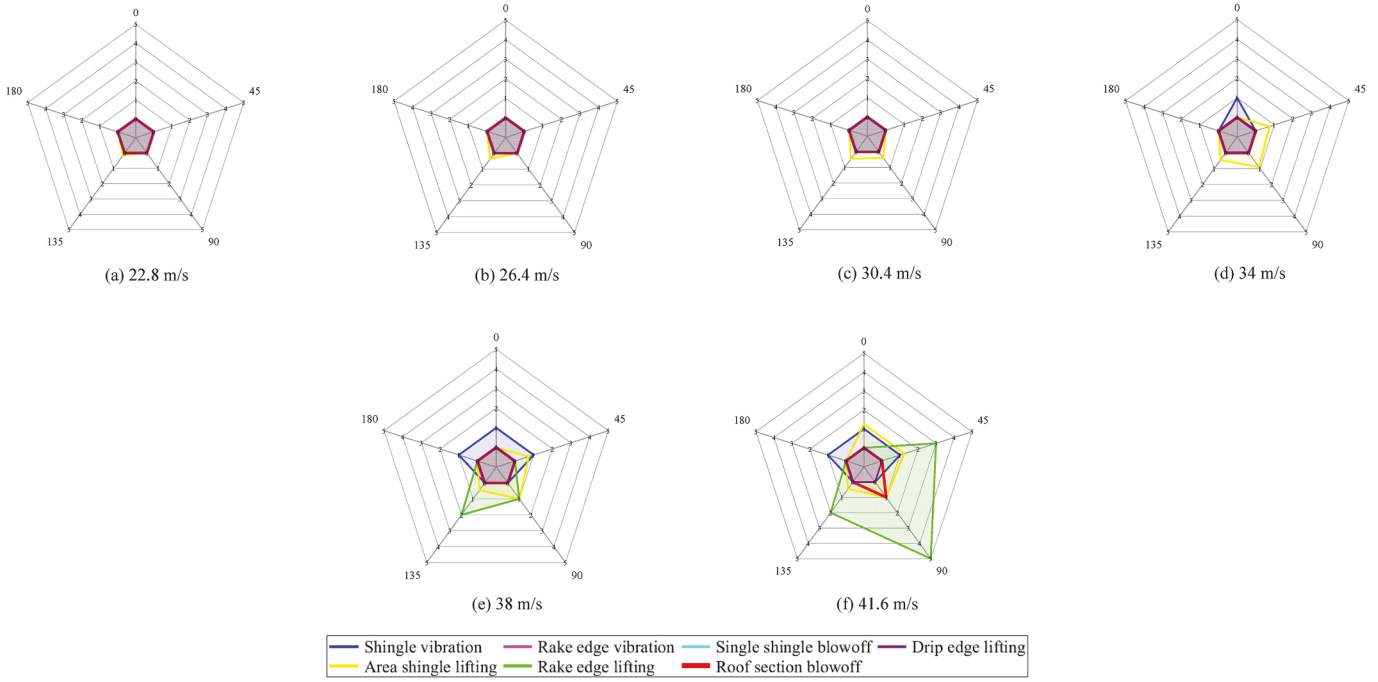

(a) 22.8 m/s (b) 26.4 m/s (c) 30.4 m/s (d) 34 m/s

(e) 38 m/s (f) 41.6 m/s

A.5. Case 3b: Hip-gable Control 2

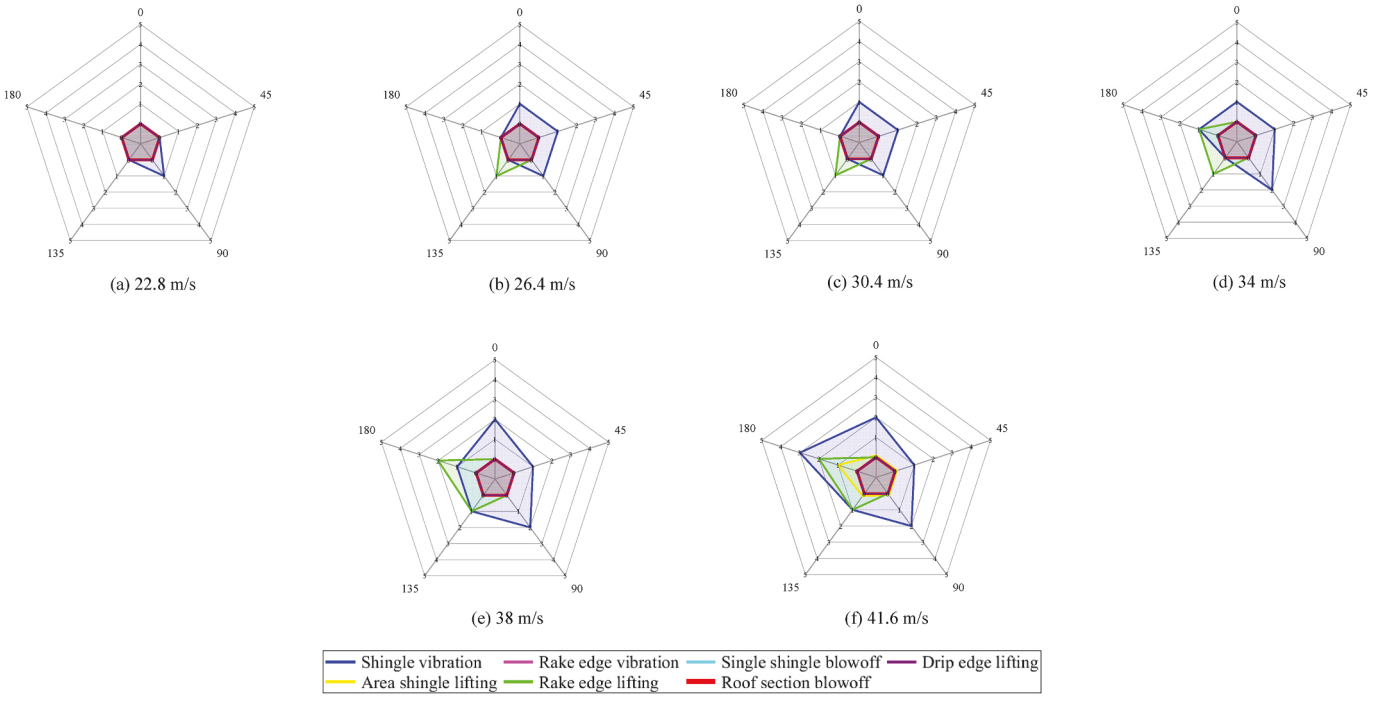

(a) 22.8 m/s (b) 26.4 m/s (c) 30.4 m/s (d) 34 m/s

(e) 38 m/s (f) 41.6 m/s

A.6. Case 4: Over-driven Nailing

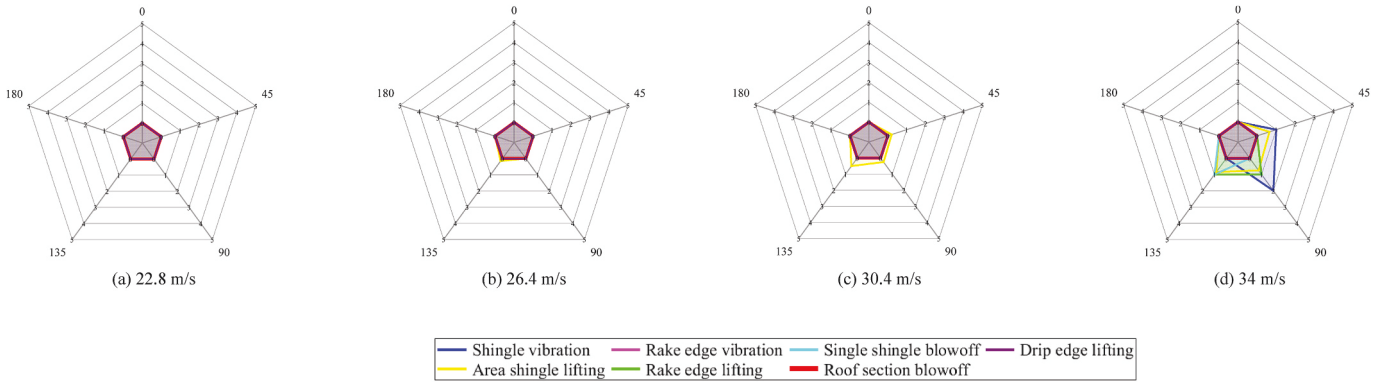

(a) 22.8 m/s (b) 26.4 m/s (c) 30.4 m/s (d) 34 m/s

A.7. Case 5: High-Nailing

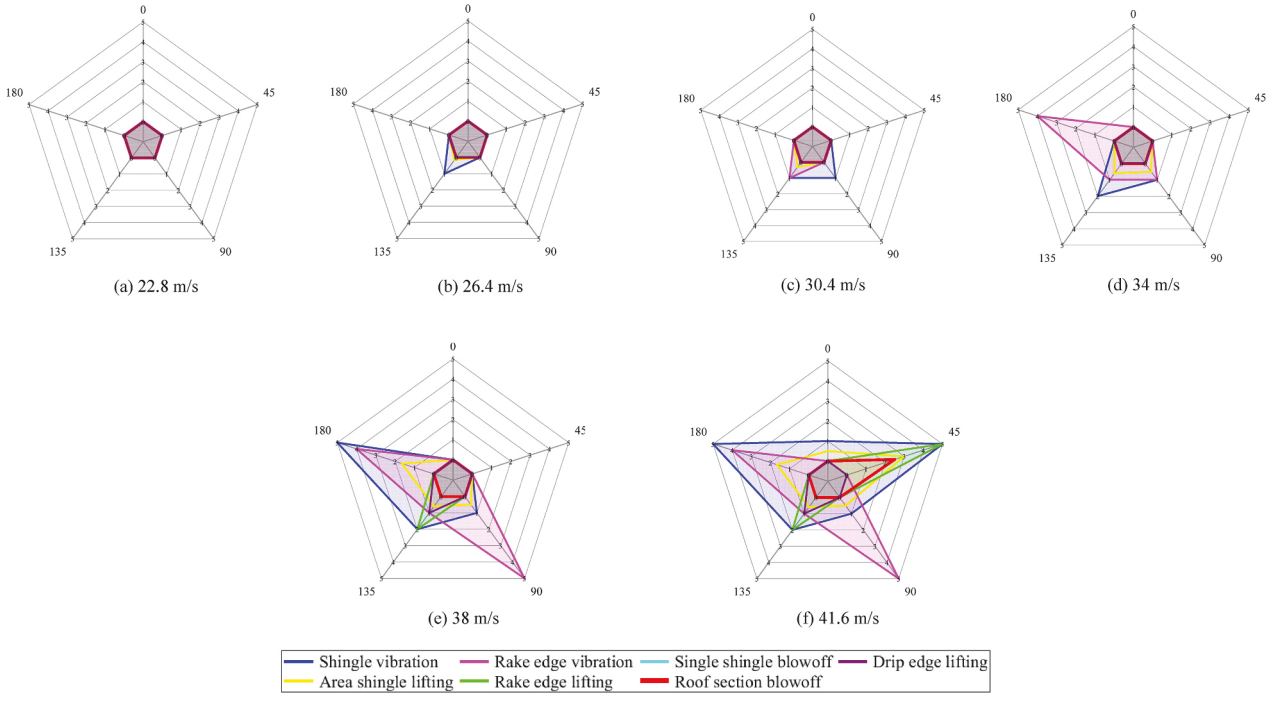

(a) 22.8 m/s (b) 26.4 m/s (c) 30.4 m/s (d) 34 m/s

(e) 38 m/s (f) 41.6 m/s

A.8. Case 6: Monoslope Control 3

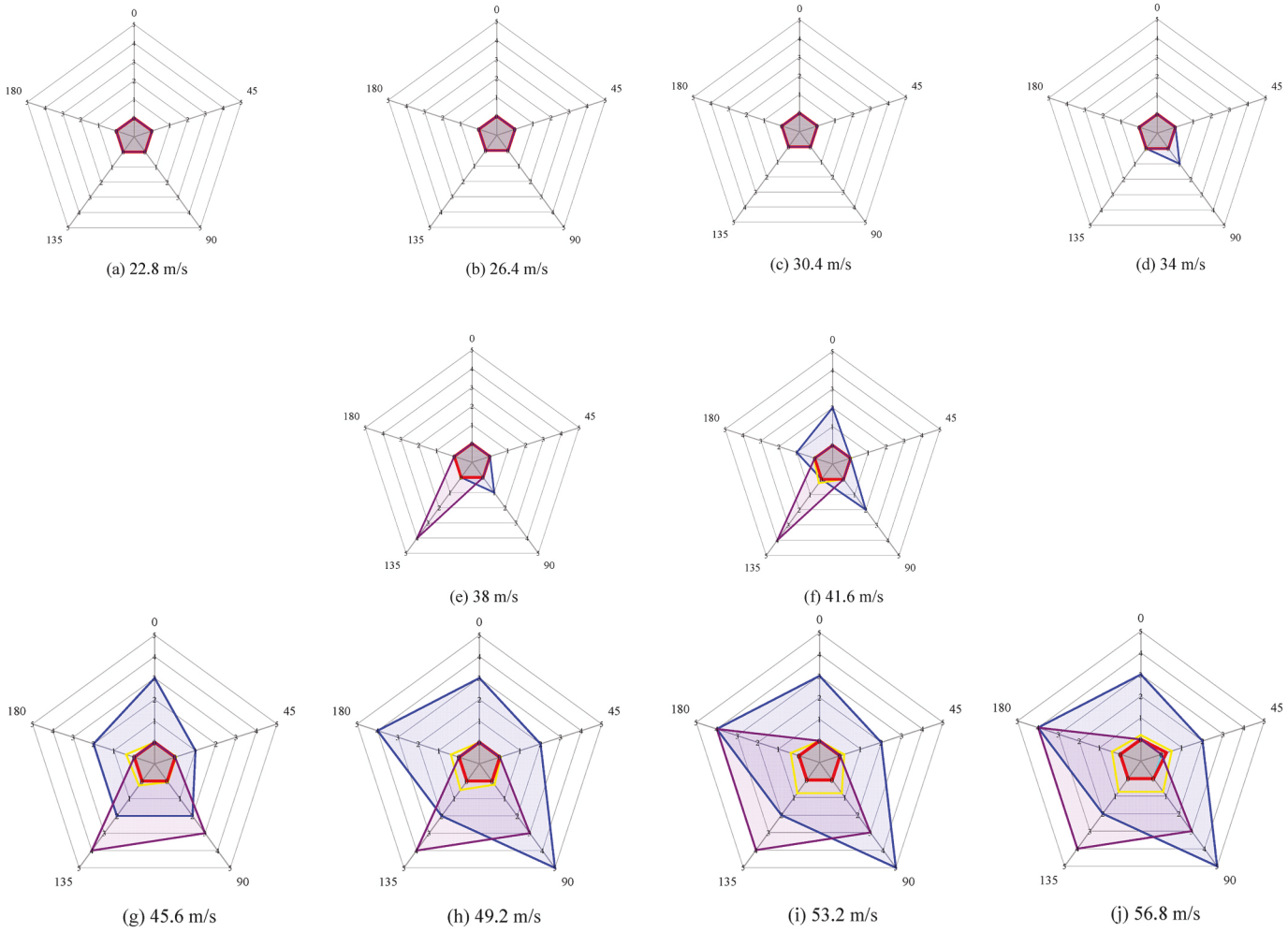

(a) 22.8 m/s (b) 26.4 m/s (c) 30.4 m/s (d) 34 m/s

(e) 38 m/s (f) 41.6 m/s

(g) 45.6 m/s (h) 49.2 m/s (i) 53.2 m/s (j) 56.8 m/s

References

Amini, M., Memari, A.M., 2020. Review of literature on performance of coastal residential buildings under hurricane conditions and lessons learned. J. Perform. Constr. Facil. 34 (6), 04020102.

ARMA, 2017. Asphalt Shingles versus Alternative & Metal Residential – Asphalt Roofing Manufacturers Association (ARMA). https://www.asphaltroofing.org/asphalt-shingles-versus-alternative-metal-residential. (Accessed 3 April 2022).

ASCE, 2021. Wind Tunnel Testing for Buildings and Other Structures. ASCE Standard. American Society of Civil Engineers (ASCE), Reston, VA, USA.

ASCE, 2022. Minimum Design Loads and Associated Criteria for Buildings and Other Structures. American Society of Civil Engineers (ASCE), Reston, VA, USA.

ASTM International, 2020a. Standard Test Method for Wind Resistance of Asphalt Shingles (Uplift Force/Uplift Resistance Method). ASTM International, West Conshohocken.

ASTM International, 2020b. Standard Test Method for Measurement of Asphalt Shingle Mechanical Uplift. ASTM International, West Conshohocken, PA.

ASTM International, 2020c. Standard Test Method for Wind Resistance of Steep Slope Roofing Products (Fan- Induced Method). ASTM International, West Conshohocken, PA.

Baheru, T., Chowdhury, A.G., Pinelli, J., 2015. Estimation of wind-driven rain intrusion through building envelope defects and breaches during tropical cyclones. Nat. Hazards Rev. 16 (2), 1–15.

Benjamin, I.A., Bono, J.A., 1967. Wind-resistance tests of roof shingles and roof assemblies. Engineering Properties of Roofing Systems 110–29.

Chowdhury, A.G., Simiu, E., Leatherman, S.P., 2009. Destructive testing under simulated hurricane effects to promote hazard mitigation. Nat. Hazards Rev. 10 (1), 1–10.

Chowdhury, A.G., Vutukuru, K.S., Moravej, M., 2018. Full- and large-scale experimentation using the wall of wind to mitigate wind loading and rain impacts on buildings and infrastructure systems. In: Proceedings of the 11th Structural Engineering Convention (SEC18). Jadavpur University, Kolkatta, India.

Chowdhury, A.G., Zisis, I., Irwin, P., Bitsuamlak, G., Pinelli, J.P., Hajra, B., Moravej, M., 2017. Large-scale experimentation using the 12-fan wall of wind to assess and mitigate hurricane wind and rain impacts on buildings and infrastructure systems. J. Struct. Eng. 143 (7), 1–16.

Cochran, L., Levitan, M., 1994. Lessons from hurricane Andrew. Architect. Sci. Rev. 37 (3), 115–121.

Cochran, L., Peterka, J., Derickson, R., 1999. Roof surface wind speed distributions on low-rise buildings roof surface wind speed distributions on low-rise buildings. Architect. Sci. Rev. 42 (3), 151–160.

Derickson, R.G., Peterka, J.A., Cermak, J.E., Cochran, L.S., 1993. Wind-tunnel Study of Shingles on a Roof (Fort Collins).

Dixon, C.R., 2013. The Wind Resistance of Asphalt Roofing Shingles. University of Florida.

Dixon, C.R., Masters, F.J., Prevatt, D.O., Gurley, K.R., 2013. Investigation of the wind resistance of asphalt shingles. Advances in Hurricane Engineering.

Dixon, C.R., Masters, F.J., Prevatt, D.O., Gurley, K.R., Brown, T.M., Peterka, J.A., Kubena, M.E., 2014. The influence of unsealing on the wind resistance of asphalt shingles. J. Wind Eng. Ind. Aerod. 130, 30–40. Elsevier.

Estephan, J., Gan Chowdhury, A., Irwin, P., 2022. A new experimental-numerical approach to estimate peak wind loads on roof-mounted photovoltaic systems by incorporating inflow turbulence and dynamic effects. Eng. Struct. 252.
Estes, H.E., Smith, J.T., Ph, D., 2017. Wind Uplift of Asphalt Shingles : Sensitivity to Roof Slope and Installation Temperature. Insurance Insitute for Business & Home Safety.
FEMA, 2004. Mitigation Assessment Team Report: Hurricane Charley in Florida.
FEMA, 2005. Mitigation Assessment Team Report: Hurricane Ivan in Alabama and Florida.
FEMA, 2006. Summary Report on Building Performance: Hurricane Katrina 2005.
FEMA, 2009. Mitigation Assessment Team Report: Hurricane Ike in Texas and Louisiana.
FEMA, 2010. Home Builder's Guide to Coastal Construction : Technical Fact Sheet Series.
FEMA, 2018. Mitigation Assessment Team Report: Hurricane Irma in Florida.
FEMA, 2019. Mitigation Assessment Team Report. Hurricane Harvey in Texas.
FEMA, 2020. Mitigation Assessment Team Report: Hurricane Michael in Florida.
Florida Building Code, 2020. 2020 Florida Building Code, Building, seventh ed. *ICC Digital Codes*. Tallahassee.
Gurley, K.R., Masters, F.J., 2011. Post-2004 hurricane field survey of residential building performance. Nat. Hazards Rev. 12 (4), 177–183.
Hazelwood, R.A., 1981. The interaction of the two principal wind forces on roof tiles. J. Wind Eng. Ind. Aerod. 8, 39–48.
IBHS, 2004. Hurricane Charley: Nature's Force vs Structural Strength.
IBHS, 2009. Hurricane Ike: Nature's Force vs Structural Strength.
Kopp, G.A., Morrison, M.J., Henderson, D.J., 2012. Full-scale testing of low-rise, residential buildings with realistic wind loads. J. Wind Eng. Ind. Aerod. 104 (106), 25–39.
Kramer, C., Gerhardt, H.J., Kuster, H.W., 1979. On the wind-loading mechanism of roofing elements. J. Ind. Aerod. 4, 415–427.
Leatherman, S.P., Chowdhury, A.G., Robertson, C.J., 2007. Wall of wind full-scale destructive testing of coastal houses and hurricane damage mitigation. J. Coast Res. 235 (5), 1211–1217.
van de Lindt, J.W., Graettinger, A., Gupta, R., Skaggs, T., Pryor, S., Fridley, K.J., 2007. Performance of wood-frame structures during hurricane Katrina. J. Perform. Constr. Facil. 21 (2), 108–116.
Liu, Z., Pogorzelski, H., Masters, F.J., Tezak, S., Reinhold, T., 2010. Surviving nature's fury: performance of asphalt shingle roofs in the real world. Interface 28 (July), 29–44.
Mooneghi, M.A., Irwin, P., Chowdhury, A.G., 2016. Partial turbulence simulation method for predicting peak wind loads on small structures and building appurtenances. J. Wind Eng. Ind. Aerod. 157, 47–62. Elsevier.
Moravej, M., 2018. Investigating Scale Effects on Analytical Methods of Predicting Peak Wind Loads on Buildings. Florida International University.
Noone, M.J., Blanchard, W.K., 1993. Asphalt shingles - a century of success and improvement. In: Proceedings of the 10th Conference on Roofing Technology.
Peterka, J.A., Cermak, J.E., 1983. Wind-tunnel Study of Wind Resistance of Roofing Shingles (Fort Collins).
Peterka, J.A., Cermak, J.E., Cochran, L.S., Cochran, B.C., Hosoya, N., Derickson, R.G., Harper, C., Jones, J., Metz, B., 1997. Wind uplift model for asphalt shingles. J. Architect. Eng. 3 (4), 147–155.
RICOWI, 2006. Hurricanes Charley and Ivan Wind Investigation Report.
RICOWI, 2007. Hurricane Katrina Wind Investigation Report.
RICOWI, 2009. Hurricanes Ike Wind Investigation Report.
RICOWI, 2018a. RICOWI Wind Investigation Hurricane Irma (Florida).
RICOWI, 2018b. RICOWI Wind Investigation Hurricane Michael (Florida).
Smith, T.L., Millen, M., 1999. Influence of Nail locations on wind resistance of unsealed asphalt shingles. Proceedings of the North American Conference on Roofing Technology 98–111.
Tolera, A.B., Mostafa, K., Chowhdury, A.G., Zisis, I., Irwin, P., 2022. Study of wind loads on asphalt shingles using full-scale experimentation. J. Wind Eng. Ind. Aerod. 225 (June), 105005. Elsevier Ltd.